Supplementary material

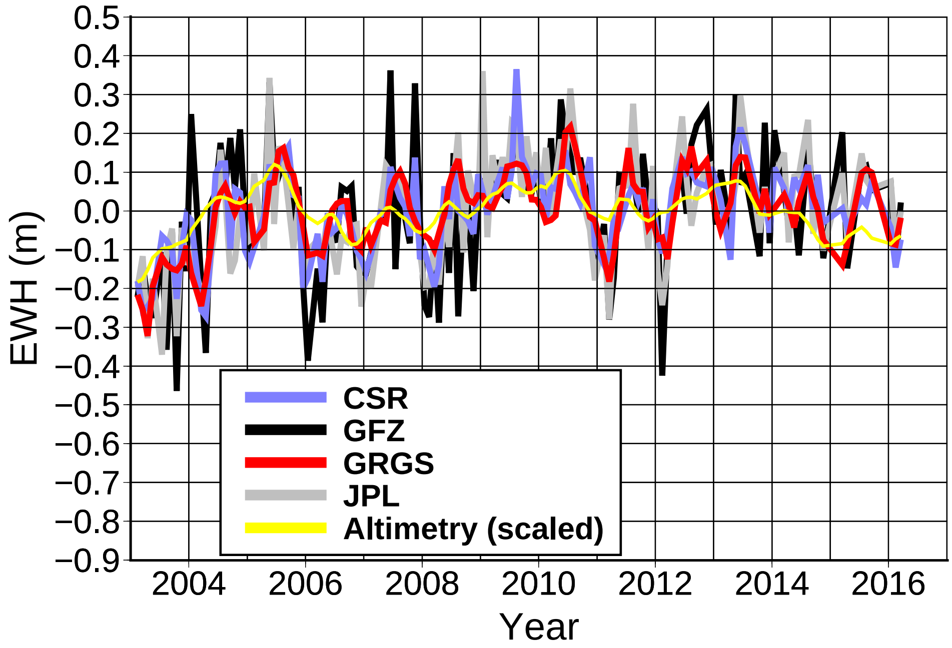

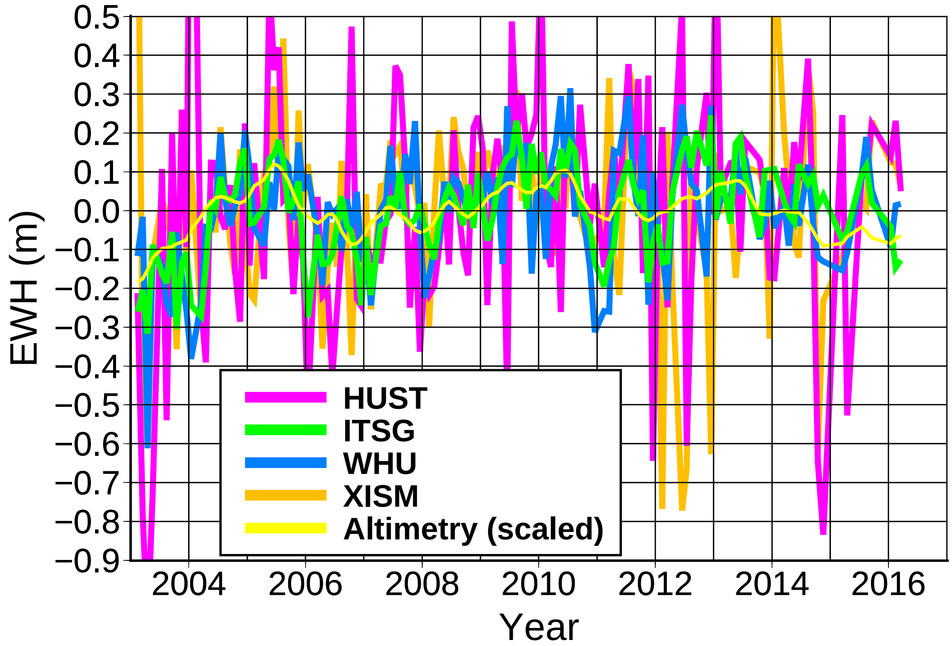

Fig. S1 GRACE-based mass anomaly time-series (in terms of EWH) versus altimetry-based water level variations in the Lake Ladoga. The latter variations are downscaled with the factor of 0.119, which is the expected signal retaining E_{exp} for the Lake Ladoga (cf. Table 2). In this way, signal damping in the GRACE solutions due to the omission error is accounted for. Each of the panels presents only four GRACE-based time-series to make each time-series better visible

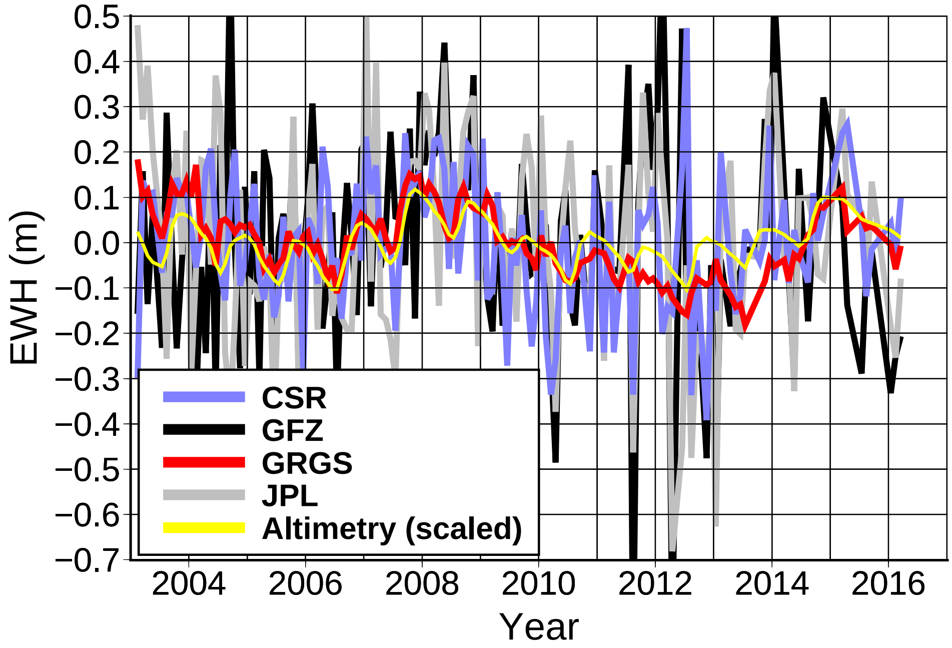

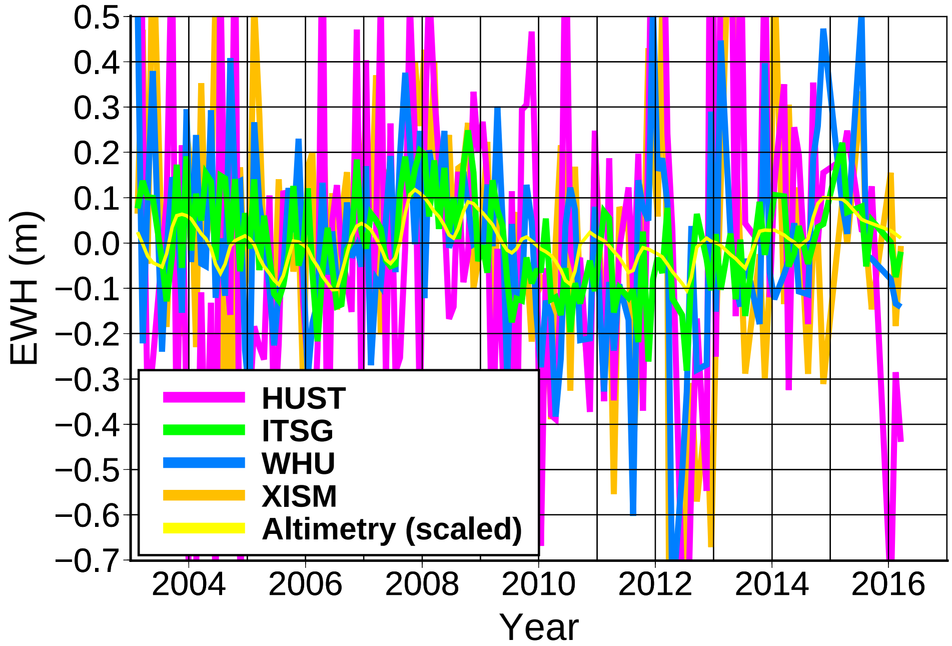

Fig. S2 Similar to Fig. S1, but for the Lake Nasser. The altimetry-based water level variations are downscaled with the factor of 0.022

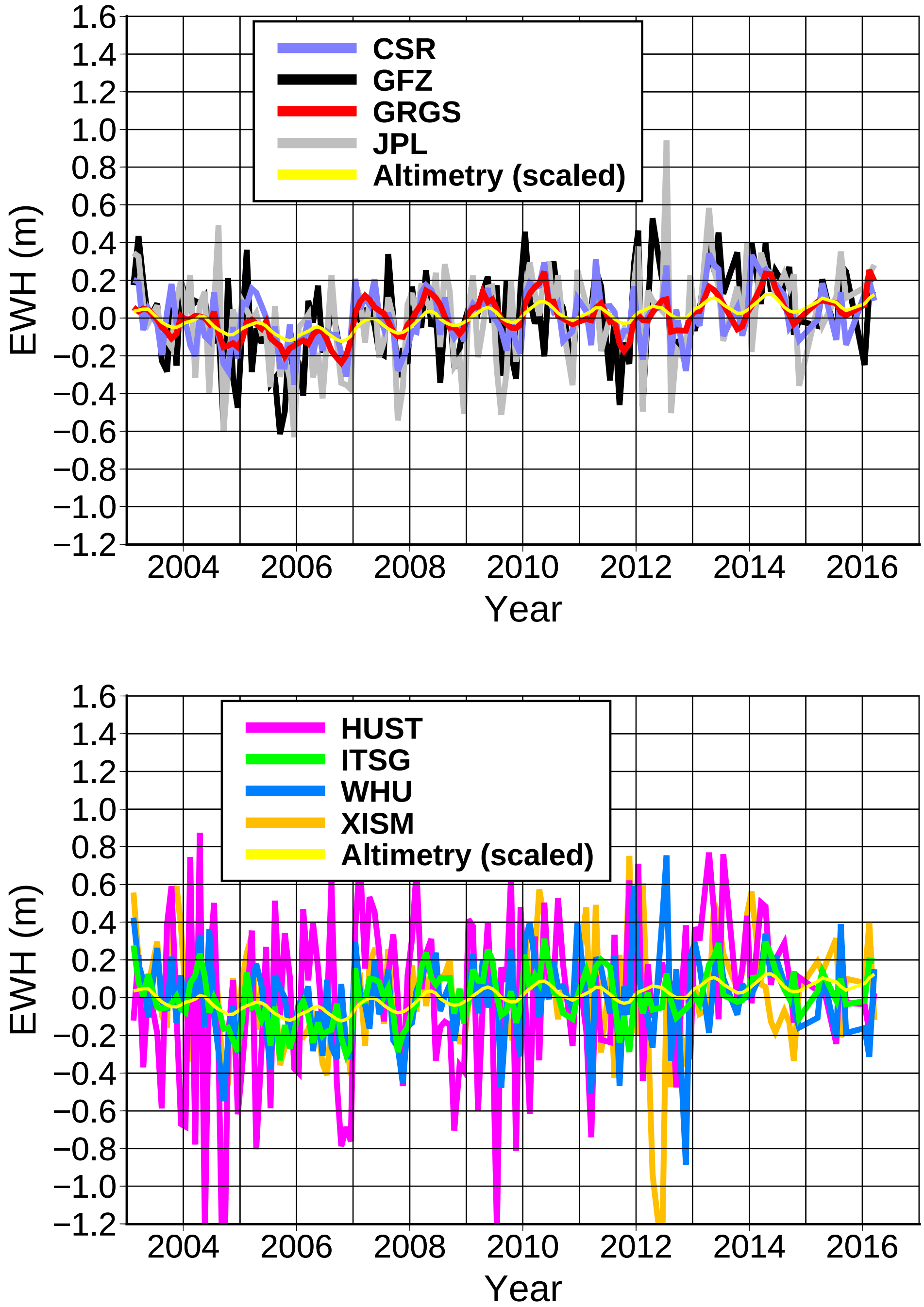

Fig. S3 Similar to Fig. S1, but for the Lake Tanganyika. The altimetry-based water level variations are downscaled with the factor of 0.141

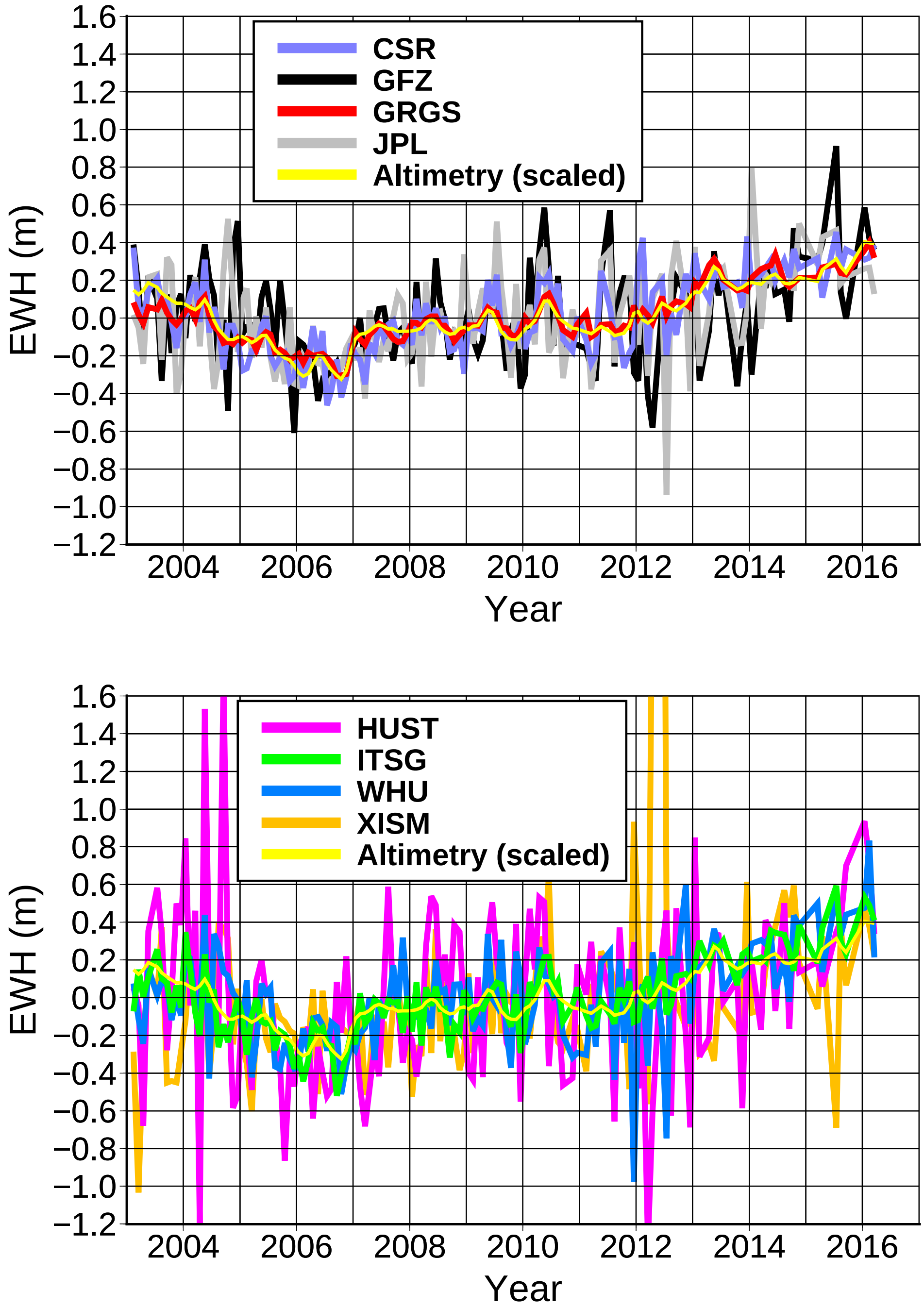

Fig. S4 Similar to Fig. S1, but for the Lake Victoria. The altimetry-based water level variations are down-scaled with the factor of 0.389

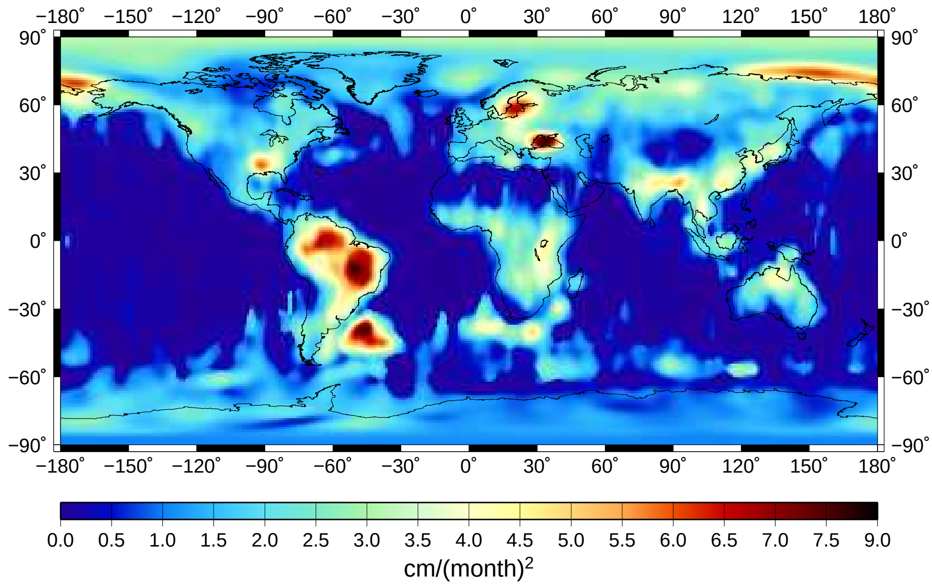

Fig. S5 Signal RMS estimated by the Variance Component Estimation in the presence of MYTD regularization (this is the value denoted as σ_s in Eq. 3). Notice that "signal RMS" in the context of the MYTD regularization refers to "non-regular" signals only, when a "regular" signal is understood as a signal composed of an annual periodic term, a linear trend, and an acceleration term. This is because the application of the MYTD regularization functional to such a regular signal results in zero. In other words, the MYTD regularization is "blind" to such a regular signal

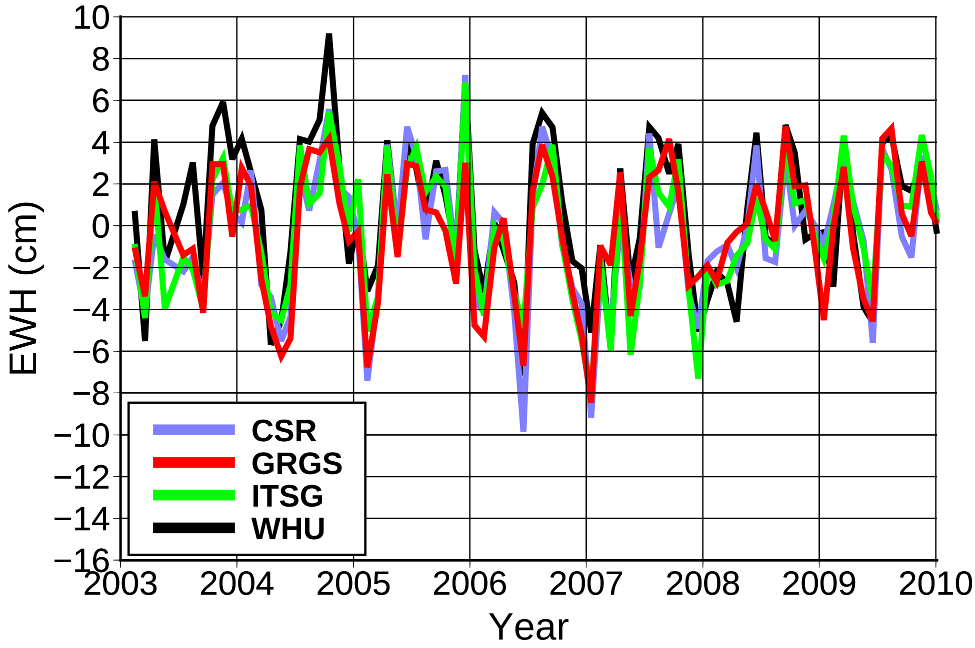

Fig. S6 Selected mass anomaly time-series at the point with coordinates $(38.5°S;\ 46.5°W)$. This is the point within the Argentine Basin where the estimated signal RMS is maximum (see Fig. S5). All the shown time-series are extracted from mass anomaly grids, which were smoothed with the Gaussian filter of 400-km half-width. In order to facilitate a visual inspection of the time-series, we limit ourselves to the time interval 2003–2010 and consider only four GRACE solution time-series with relatively low noise levels (CSR, GRGS, ITSG, and WHU)

(a)

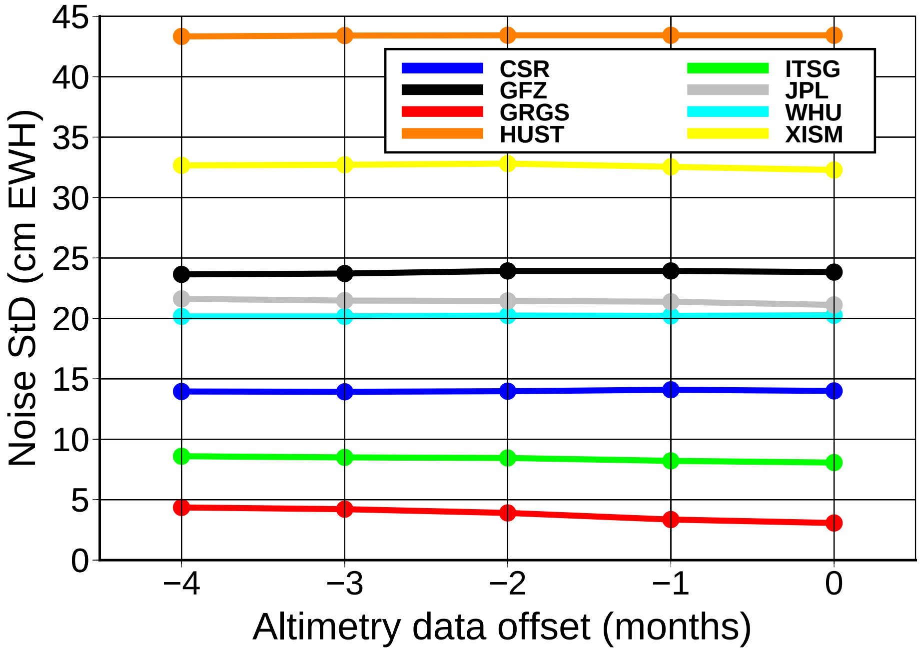

(b)

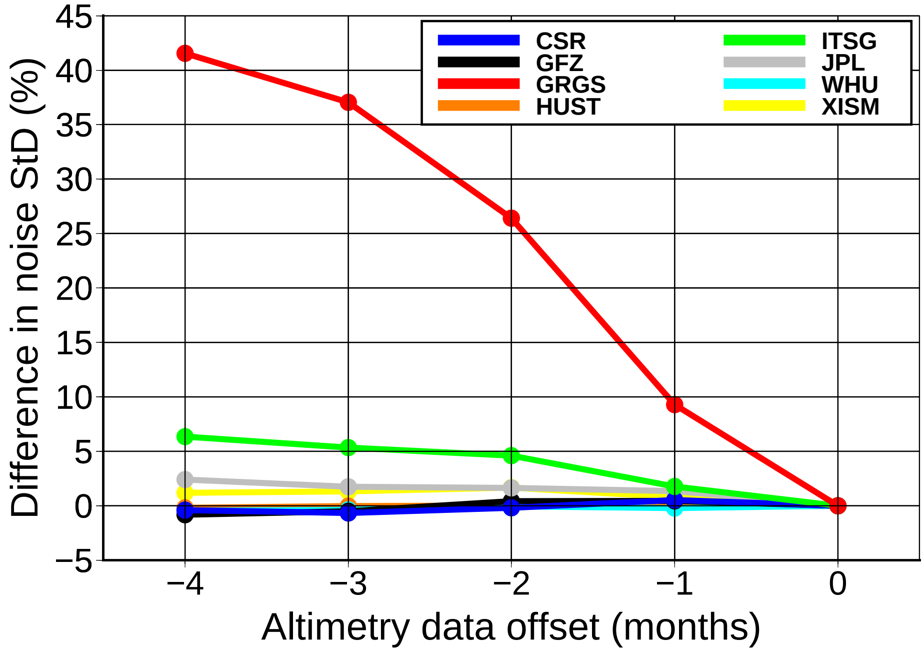

Fig. S7 Top panel: estimated standard deviations of noise in the GRACE-based mass anomaly time-series over lake Nasser after applying a time offset to altimetry data (negative numbers reflect the fact that the altimetry data are offset back in time). Bottom panel: similar to the top one, but relative differences of the estimated noise StDs are shown instead of noise StDs themselves. The differences are computed as $(\sigma_k - \sigma_0)/\sigma_0 \times 100\%$, where σ_k is the estimated noise StD after applying the offset of k months to the altimetry data and σ_0 is the noise StD estimated from the original altimetry data

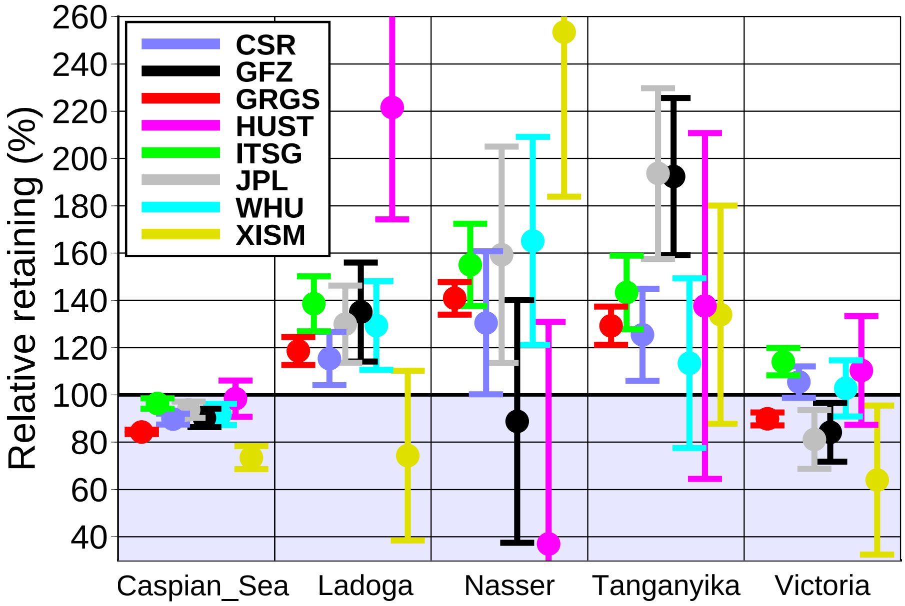

Fig. S8 Relative signal retainings of the GRACE-based mass anomaly time-series over the five considered lakes: same as Fig. 6, but without the GLDAS-based correction for the leakage of hydrological signals

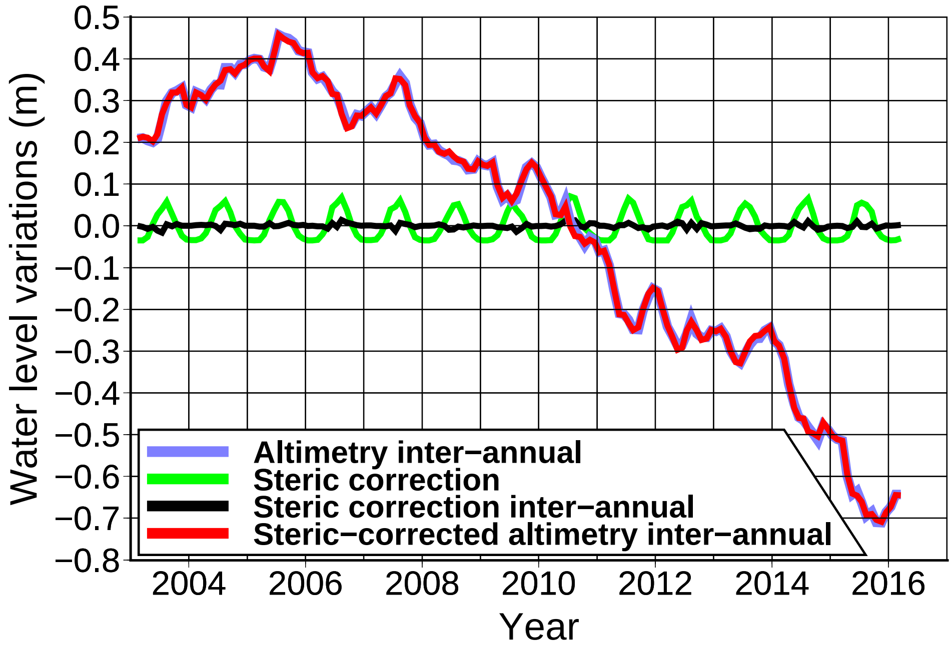

Fig. S9 Water level variations in the Caspian Sea. Steric component computed from the mean water temperature variations at eight selected stations: original (in green) and obtained after the subtraction of annual and semi-annual periodic component (in black); total inter-annual water level variations obtained after the subtraction of annual and semi-annual periodic component: original (in blue) and after the subtraction of the steric signal (in red)